Palaeogeography, Palaeoclimatology, Palaeoecology 281 (2009) 363–375

Contents lists available at ScienceDirect

Palaeogeography, Palaeoclimatology, Palaeoecology

journal homepage: www.elsevier.com/locate/palaeo

Palaeoenvironmental changes during the last 1600 years inferred from the sediment record of a cirque lake in southern Patagonia (Laguna Las Vizcachas, Argentina)

Michael Fey [a,*], Christian Korr [a], Nora I. Maidana [b], María L. Carrevedo [b], Hugo Corbella [c], Sara Dietrich [d,e], Torsten Haberzettl [f], Gerhard Kuhn [g], Andreas Lücke [e], Christoph Mayr [h], Christian Ohlendorf [a], Marta M. Paez [i], Flavia A. Quintana [i], Frank Schäbitz [d], Bernd Zolitschka [a]

[a] Universität Bremen, Institut für Geographie, GEOPOLAR–Geomorphologie und Polarforschung, Celsiusstr. FVG-M, 28359 Bremen, Germany
[b] Universidad Nacional de Buenos Aires–CONICET, Departamento de Biodiversidad y Biología Experimental, Ciudad Universitaria, C1428EHA, Buenos Aires, Argentina
[c] Museo Argentino de Ciencias Naturales Bernardino Rivadavia, Av. Angel Gallardo 470, C1405DJR, Buenos Aires, Argentina
[d] Universität zu Köln, Seminar für Geographie und ihre Didaktik, Gronewaldstr. 2, 50931 Köln, Germany
[e] Forschungszentrum Jülich, Institut für Chemie und Dynamik der Geosphäre, ICG-V: Sedimentäre Systeme, 52425 Jülich, Germany
[f] Université du Québec à Rimouski, Institut des sciences de la mer de Rimouski (ISMER), 310 allée des Ursulines, Rimouski, Québec, Canada G5L 3A1
[g] Alfred-Wegener-Institut für Polar- und Meeresforschung, Am Alten Hafen 26, 27568 Bremerhaven, Germany
[h] Ludwig-Maximilians-Universität München, GeoBio-Center[LMU] und Department für Geo- und Umweltwissenschaften, Richard-Wagner-Str. 10, 80333 München, Germany
[i] Universidad Nacional de Mar del Plata, Departamento de Biología, Laboratorio de Paleoecología y Palinología, Funes 3250, 7600 Mar del Plata, Argentina

ARTICLE INFO

Article history:
Received 15 July 2007
Accepted 11 January 2009
Available online 9 April 2009

Keywords:
Lake sediments
Geochemistry
Diatoms
Palaeoclimatology
'Medieval Climate Anomaly'
'Little Ice Age'
Patagonia

ABSTRACT

Laguna Las Vizcachas is a cirque lake located at the margin of an extra-Andean volcanic plateau in southern Patagonia, Argentina, within the area of steppe and semi-desert east of the Andes. The number of paleoenvironmental records is still limited in this region. Sediments of this lake were studied in order to obtain multi-proxy information about the paleoenvironmental history of this site for the 'Medieval Climate Anomaly' and the 'Little Ice Age' chronozones. In combination with results from other sites across southern Patagonia, our data enhance the understanding of spatial patterns of past hydrological changes and contribute to distinguishing between the signals of temperature and precipitation. As Laguna Las Vizcachas is situated at 1100 m a.s.l. in a cool 'mountain climate', the lake system is more sensitive to changes of temperature and winter ice cover than other sites from lower elevations in this region. Our interpretation of the multi-proxy dataset is based on signals of clastic sediment input, lake productivity, organic matter sources and preservation, dilution effects and early diagenetic overprint. The record reveals a period of enhanced fluvial runoff resulting from higher precipitation from the 12th until the end of the 14th century as inferred from high concentrations of Ti, Ca, and from magnetic susceptibility. This may coincide with higher wind intensities as suggested by higher proportions of epiphytic diatoms which point to an enhanced lateral transport from their littoral habitat towards the coring position at the center of the lake. In comparison with other records from southern Patagonia, the results from Laguna Las Vizcachas suggest opposite precipitation regimes between the western and eastern parts of Patagonia during that time which corresponds partly to the 'Medieval Climate Anomaly' chronozone. However, this proposal is compromised by the chronological uncertainties of the different records under consideration. The diatom record of Laguna Las Vizcachas indicates temperature changes: highest proportions of benthic diatoms point to coldest conditions from the mid-15th until the mid-17th century, followed by relatively warm conditions until the mid-18th century as suggested by a decrease of benthic taxa and a conspicuous rise of the planktonic/non-planktonic diatom ratio that can be used as an indicator for the length or presence/absence of winter ice cover.

1. Introduction

Patagonia is the southernmost continental landmass in the southern hemisphere except for Antarctica. Hence, it provides the unique opportunity to obtain terrestrial palaeoclimate data from the higher southern mid-latitudes which are subject to shifts in polar and mid-latitude pressure fields and precipitation regimes (Weischet, 1996; Paruelo et al., 1998). The environmental conditions are characterized by intense interactions between terrestrial, marine and glacial influences as a consequence of the peculiar geographical setting within the vast southern oceans and in relative proximity to Antarctica (Zolitschka et al., 2006). In combination with marine and terrestrial records from southern, tropical and northern latitudes, palaeoclimate reconstructions from southern Patagonia will contribute to a better

* Corresponding author. Tel.: +49 421 218 67154; fax: +49 421 218 67151.
E-mail address: fey@uni-bremen.de (M. Fey).

0031-0182/$ – see front matter © 2009 Elsevier B.V. All rights reserved.
doi:10.1016/j.palaeo.2009.01.012

understanding of the global climate system, i.e., to detect teleconnections and to reveal large-scale spatial and temporal patterns of climate changes. In addition, they may help to validate output of climate models (e.g., Wagner et al., 2007).

Until today most palaeoecological and palaeoclimate investigations in southern Patagonia and adjacent Tierra del Fuego archipelago have focused on pollen and charcoal studies of peat bogs and mires from the Andes and the forest–steppe ecotone (e.g., Heusser, 1993, 1995, 1998; McCulloch and Davies, 2001; Huber and Markgraf, 2003; Fesq-Martin et al., 2004; Huber et al., 2004), while terrestrial records from the steppes and semi-deserts east of the Andes are scarce. The latter are represented by palynological studies at archeological sites (e.g., Mancini, 1998; Prieto et al., 1998; Mancini et al., 2005) and multi-proxy investigations of sediments from Lago Cardiel (Fig. 1) (Markgraf et al., 2003; Gilli et al., 2005a,b). Recently published results of high-resolution studies of crater lake sediments from the Pali Aike Volcanic Field (Fig. 1) in south-eastern Patagonia supported by studies of modern lake systems have added valuable multi-proxy information. Laguna Potrok Aike (Fig. 1), in particular, has turned out to be extremely sensitive to hydrological changes (Schäbitz et al., 2003; Haberzettl et al., 2005; Mayr et al., 2005; Haberzettl et al., 2006; Zolitschka et al., 2006, Haberzettl et al., 2007; Mayr et al., 2007a,b; Wille et al., 2007; Haberzettl et al., 2008). However, spatial patterns of the inferred hydrological changes remain speculative. Hence, there is a need for additional palaeoclimate information from other parts of southern Patagonia, especially from further west, i.e., from the area between Laguna Potrok Aike and the Andean Cordillera. In addition, records from the Pali Aike Volcanic Field are derived from rather low altitudes while palaeoclimate data from extra-Andean high elevation sites might be more sensitive to temperature changes.

The multi-proxy study of lacustrine sediments from the extra-Andean Meseta de las Vizcachas (Fig. 1) presented here aims to fill this gap.

2. Site description

The cirque lake Laguna Las Vizcachas (VIZ) is located at 50°42′S, 71°59′W about 60 km SE of the town of El Calafate in the Santa Cruz Province, southern Patagonia, Argentina (Fig. 1). It is situated at about 1100 m a.s.l. in front of a steep cliff which forms the headwall of the cirque at the southern margin of the basalt plateau Meseta de las Vizcachas. This plateau reaches elevations of about 1400 m a.s.l. and is probably of Pliocene age (Schellmann, 1998). The age of the cirque formation is unknown. While the ice shield of the Last Glaciation did probably not reach the area, it is likely that local glaciers were present during that time (Wenzens, 1999, 2004). Today there are no glaciers in the area. The lake exhibits an irregular shape and bathymetry; it extends about 1300 m from north to south and 600 m from west to east with a maximum water depth of 19 m (Fig. 1). A hummocky relief formed by glacial moraines characterizes the surrounding area. The lake is fed by a stream draining the plateau and entering the lake via a waterfall on the northwestern shore. An outflow is situated at the southern end of the lake (Fig. 1). The modern vegetation around Laguna Las Vizcachas is classified as *Festuca pallescens* grass steppe of the Sub-Andean district of the Patagonian Phytogeographic Province (León et al., 1998). Due to the remoteness of the area, local meteorological data are not available. However, regional interpolation suggest an annual precipitation rate of around 300 mm (Hoffman, 1975; Oliva et al., 2001). Based on temperature data from the Lago Argentino meteorological station (50°20′S, 72°18′W; 220 m a.s.l.) (Sträßer, 1999) near the town of El Calafate (Fig. 1), mean monthly air temperatures are estimated to range between 3.1 and 7.1 °C for January and from −9.3 to −5.3 °C for July. Observational data about ice cover on the lake in winter are not available; the lake is too small to get this information from satellite images. However, the temperature estimates suggest that Laguna Las Vizcachas is frozen for several months of the year. This is supported by the fact that even the crater lake Laguna Azul in south-eastern Patagonia (Fig. 1), which is situated at only 100 m a.s.l. (Zolitschka et al., 2006) and located closer to the influence of the Atlantic Ocean, is commonly ice-covered for about one month in winter (Gabriel Oliva, pers. comm., 2006). Hence, ice cover on Laguna Las Vizcachas at 1100 m a.s.l. is expected to persist considerably longer. The local topography favors ice cover at Laguna Las Vizcachas as the steep cliff to the east, north and north-west (Fig. 1) diminishes solar irradiation especially in winter when the sun is below the local skyline. Similar effects were observed at a cirque

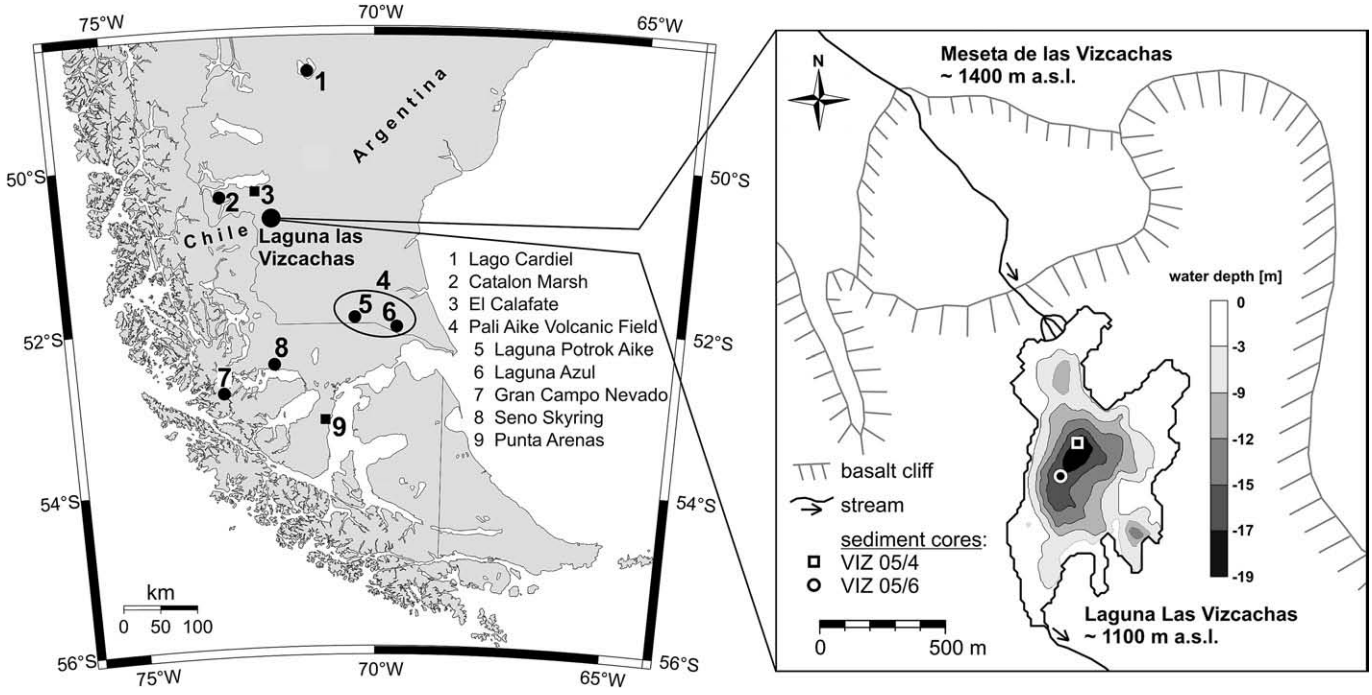

Fig. 1. Research area in southern South America and locations mentioned in the text. The map was created with Online Map Creation, http://www.aquarius.geomar.de/omc/ (left). Bathymetry of Laguna Las Vizcachas, coring positions and surrounding local topography (right).

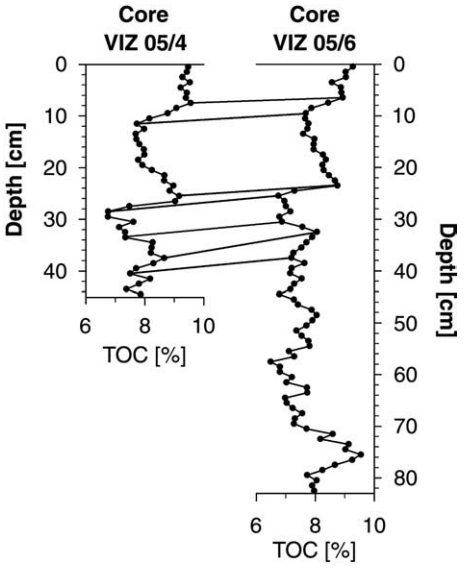

Fig. 2. Good correlation between the sediment cores VIZ 05/4 and VIZ 05/6 from the central basin of Laguna Las Vizcachas as evidenced by the records of total organic carbon (TOC). Lines between records demonstrate corresponding TOC wiggles. For coring positions see Fig. 1.

lake in the Swiss Alps (2339 m a.s.l.) where mean monthly air temperature values are comparable to the estimates for Laguna Las Vizcachas (Ohlendorf et al., 2000). Measurements of physico–chemical properties of the surface water of Laguna Las Vizcachas conducted in March (late summer) 2005 revealed a water temperature of 6.9 °C, an electric conductivity of 55 µS cm^{-1} and a pH of 7.7. Thus the measured water temperature is in close agreement with the air temperature estimates.

3. Material and methods

3.1. Coring and sampling

During March 2005 six short sediment cores were recovered from different positions on Laguna Las Vizcachas (Fig. 1). Five cores, 44–83 cm in length, were taken from the central basin of the lake. One 35 cm long core was retrieved from the shallower south-eastern sub-basin. Sediment cores were sealed gas-tight and transported to the GEOPOLAR Core Repository, Bremen (Germany), where they were stored cool and dark until subsampling. Here we present results of the 83 cm long sediment core VIZ 05/6 from the lake's central basin (50°42.39′S, 71°58.64′W; 16 m water depth; Fig. 1) which was obtained with a modified ETH-gravity corer (Kelts et al., 1986). This core was chosen for further analyses as it was by far the longest of the six cores and its location suggests it would be well suited to represent pelagic sedimentation. In order to verify whether this core is representative of the central basin of the lake, analyses of selected parameters as described below (e.g., magnetic susceptibility, total organic carbon, total nitrogen) were also performed on a second but shorter (45 cm) core from the lake center (VIZ 05/4, 18 m water depth; Fig. 1). This core was retrieved with a Kajak-type gravity corer and had already been sampled in the field. Both cores showed good correlation (Fig. 2) suggesting continuous sediment accumulation. In this paper, only the results of the longer core VIZ 05/6 will be reported. The core was split, photographed, lithologically described, and smear slides were prepared from selected depths for microscopic investigation. After employing non-destructive logging techniques (magnetic susceptibility, XRF elemental analysis; see below) the core was sub-sampled volumetrically in continuous 1 cm intervals. Aliquots from each sub-sample were divided for different analytical procedures. All analyses were carried out at 1 cm resolution, except for diatom analysis which was performed at 4 cm resolution.

3.2. Chronology

Radiocarbon ages of seven samples were determined by AMS ^{14}C dating techniques at the Poznań Radiocarbon Laboratory, Poland (Table 1). The fine fraction (<100 µm) of bulk sediment was dated, while aquatic macrophyte remains were avoided as they were considered to possibly represent layers of reworked material. Radiocarbon ages were calibrated with the southern hemisphere calibration curve (shcal04, McCormac et al., 2004) using the software CALIB 5.0.2 (Stuiver and Reimer, 1993; Stuiver et al., 2005). One post-modern age was calibrated with the software CALIBomb (Reimer et al., 2004) applying the southern hemisphere data set (Hua and Barbetti, 2004). All ages are given in calendar years AD.

3.3. Physical properties and mineralogy

Water content (WC) and dry density (DD) were calculated from the fresh and freeze-dried volumetric sub-sample weights. Volume specific magnetic susceptibility (κ) was measured on the split core in 1 cm increments with a Bartington F-sensor employed on a measuring bench developed by the Department of Marine Geophysics, University of Bremen (Dearing, 1994; Nowaczyk, 2001). Values are given in 10^{-6} SI (dimensionless). The mineralogical composition of selected samples was determined by standard powder X-ray diffraction (XRD) analyses (Philips X'Pert Pro MD equipped with an X'Celerator Detector Array).

Table 1
AMS radiocarbon dates from Laguna Las Vizcachas (core VIZ 05/6).

Sediment depth [cm]	Sample type	Lab. no.	Radiocarbon age [^{14}C BP ± 1σ]	Calibration program	Calibration curve	Calibrated age median probability [cal. AD]	Calibrated age 2σ minimum [cal. AD]	Calibrated age 2σ maximum [cal. AD]
6.0–7.0	Fraction <100 µm[a]	Poz-17477	102.66 ± 0.38 pMC[b]	CALIBomb[c]	SH1[e]	1956.68[g]	1957.50	1955.85
20.0–21.0	Fraction <100 µm[a]	Poz-17518	525 ± 30	CALIB 5.0.2[d]	SHCal04[f]	1430[h]	1450[h]	1405[h]
30.0–31.0	Fraction <100 µm[a]	Poz-12443	515 ± 30	CALIB 5.0.2[d]	SHCal04[f]	1435[h]	1455[h]	1410[h]
54.0–55.0	Fraction <100 µm[a]	Poz-12402	660 ± 30	CALIB 5.0.2[d]	SHCal04[f]	1345	1400	1300
64.0–65.0	Fraction <100 µm[a]	Poz-17519	1075 ± 30	CALIB 5.0.2[d]	SHCal04[f]	1010	1130	905
73.0–74.0	Fraction <100 µm[a]	Poz-17478	1460 ± 30	CALIB 5.0.2[d]	SHCal04[f]	635	670	585
81.5–82.5	Fraction <100 µm[a]	Poz-12403	1695 ± 30	CALIB 5.0.2[d]	SHCal04[f]	415	535	270

[a] Fine fraction of bulk sediment.
[b] pMC: percent modern carbon.
[c] Reimer et al., 2004.
[d] Stuiver and Reimer, 1993; Stuiver et al., 2005.
[e] Hua and Barbetti, 2004.
[f] McCormac et al., 2004.
[g] Mean of 2σ ranges of post-bomb calibration.
[h] Date excluded from age–depth model, probably containing reworked organic matter.

3.4. Stable isotopes

Sub-samples for isotopic analyses of organic carbon ($\delta^{13}C_{org}$) were freeze-dried, homogenized and sieved with a 200 µm sieve to eliminate macrophyte debris. Thereafter, samples were decarbonized with HCl (5%) for 6 hours in a water bath at 50 °C, and then centrifuged, rinsed repeatedly with deionized water to neutralize pH, and freeze-dried. Isotope ratios were determined on approximately 1.0–1.5 mg of sample weighted into tin capsules and combusted at 1080 °C in an elemental analyzer (EuroEA, Eurovector) with automated sample supply linked to an isotope ratio mass spectrometer (Isoprime, Micromass). Isotope ratios are reported as δ values in per mil according to the equation

$$\delta = (R_s / R_{st} - 1)*1000 \quad (1)$$

with R_s and R_{st} as isotope ratios ($^{13}C/^{12}C$) of the samples and the international standard (VPDB), respectively. Analytical uncertainty (one standard deviation) is 0.08‰.

3.5. Geochemistry

Element measurement were obtained from the split core with 1 cm resolution using an Avaatech X-ray Fluorescence (XRF) core scanner (Zolitschka et al., 2001; Richter et al., 2006; Tjallingii et al., 2007) at the Alfred Wegener Institute for Polar and Marine Research, Bremerhaven. Values are given in total counts (cnts). Total carbon (TC), total nitrogen (TN) and total sulfur (TS) were measured with a CNS elemental analyzer (EuroEA, Eurovector). Prior to their measurement freeze-dried sub-samples were ground in a mortar and homogenized after picking out macro-remains. Concentrations of total organic carbon (TOC) were determined with the same device after successive treatment with 3% and 20% HCl at 80 °C in order to remove carbonates. Total inorganic carbon (TIC) was calculated as the difference between TC and TOC.

Biogenic silica (BiSi) was analyzed by applying an alkaline digestion in autoclaves and subsequent detection by a continuous flow system with UV–VIS spectroscopy. Six to eight milligrams of sample material were weighted into Teflon®-autoclaves. After addition of 20 ml 1 M NaOH, digestion was performed for 120 min at 100 °C in a pressure pulping system. The resulting solution was filtered and an aliquot of 5 ml was diluted with 20 ml 1 M NaOH in order to determine BiSi passing the continuous flow system with UV–VIS spectroscopy. The resulting values were in good agreement with measurements made with the conventional automated leaching method (Müller and Schneider, 1993). The pressure pulping method yields even better reproducibility with significantly lower standard deviations and has a higher sample capacity. Hence, all BiSi values

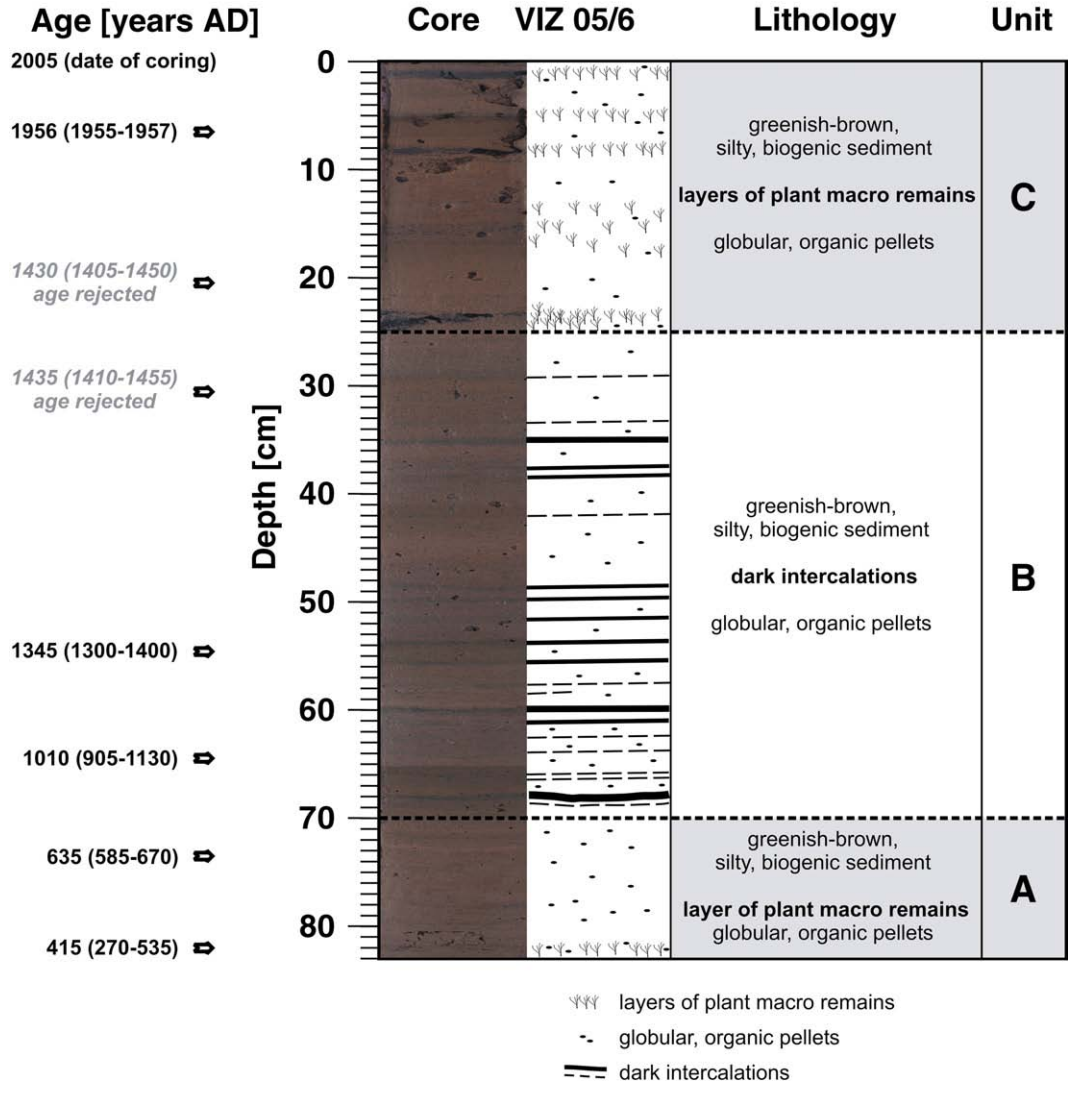

Fig. 3. Lithology of core VIZ 05/6 from Laguna Las Vizcachas and radiocarbon dates (median probability, 2σ range of calibration in brackets).

which are reported in the following were determined with this method. This method should, however, be applied only on organic rich sediments such as those of Laguna Las Vizcachas, as siliciclastic components may lead to an overestimation of BiSi due to partial dissolution of minerogenic silica.

Correlations are reported using the Spearman–Rho correlation coefficient (r_s), which represents a more robust measure than the frequently used Pearson correlation coefficient (r) as it is also applicable to non-linear relationships and/or populations with a non-Gaussian distribution (Fowler et al., 1998).

3.6. Diatoms

Samples were heated with hydrogen peroxide to oxidize organic material and mounted onto microscope slides following standard procedures (Battarbee, 1986). Duplicated permanent slides for light microscopy were prepared with Naphrax®. A minimum of 400 valves per slide were counted in order to calculate relative frequencies. Identification of diatom taxa to species level or variety is based on standard literature (e.g., Krammer and Lange-Bertalot, 1986; Simonsen, 1987; Krammer and Lange-Bertalot, 1988, 1991a,b; Rumrich et al., 2000). Taxonomic nomenclature follows criteria set up by Round et al. (1990). Ecological characteristics were taken from Lowe (1974), De Wolf (1982) and van Dam et al. (1994).

4. Results

4.1. Lithology

The sediments of core VIZ 05/6 consist of homogeneous to faintly laminated, greenish-brown, silty, biogenic sediment with small, black, globular, organic pellets. Based on the presence or absence of dark intercalations or layers of fibrous plant macro-remains, the core was subdivided into three lithological units: unit A 83–70 cm, unit B 70–25 cm and unit C 25–0 cm (Fig. 3). Unit A exhibits no dark intercalations, but a layer of plant macro-remains at 82 cm sediment depth. Unit B is characterized by the presence of many dark intercalations and unit C features layers of plant macro-remains at 0.5–1.5 cm, 4.5–5.5 cm, 7.5–8.5 cm, 13.0–16.5 cm and 23.0–25.0 cm sediment depth (Fig. 3).

4.2. Chronology

The age control for the 83 cm long core is based on seven AMS ^{14}C dates revealing ages between AD 1957 and AD 410 (Table 1). The age–depth model is constructed by linear interpolation between the sediment/water interface (March 2005) and dating results (Fig. 4). It interpolates between the medians of the probability density functions of pre-bomb calibration and the 2σ range mean of post-bomb calibration (Table 1). The comparatively young (i.e., post-modern) age of the uppermost dating sample between 6 and 7 cm sediment depth suggests that there is no reservoir effect. A hard-water effect is also not expected as the catchment area is located on the basalt plateau of the Meseta de las Vizcachas. Ages for depths below the lowermost dating sample were obtained by extrapolation of the sedimentation rate. Accordingly, the sediment record reaches a basal age of AD 390 (Figs. 4, 5). Two dates were rejected as they show almost identical ages (~AD 1430) within 10 cm depth difference. This is unrealistic in light of the general age–depth relations within the record and because there is no hint for rapid sedimentation or a slump at that sediment depth as evidenced by both cores VIZ 05/4 and VIZ 05/6 from different positions within the lake center (Figs. 1, 2). More likely, these two dates result from synsedimentary contamination by reworked 'old' carbon which may point to erosion of older sediment strata due to wave action near the shore. Rejection of the two dates and linear interpolation leads to a slightly enhanced age uncertainty in this section, while the age–depth model is more reliable in the sections above and below due to a shorter depth distance between the accepted dating samples (Fig. 4). In the following, all data are reported and discussed according to the age–depth model presented in Fig. 4. Sedimentation rates (SR) vary between 0.24 and 0.38 mm a^{-1} in the lower part and between 0.78 and 1.35 mm a^{-1} in the upper part of the record (Fig. 5).

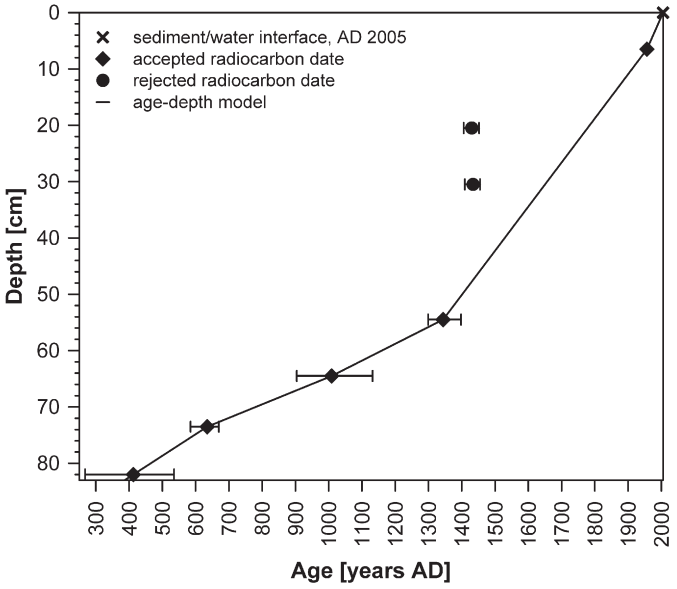

Fig. 4. Age–depth model for the core VIZ 05/6 from Laguna Las Vizcachas. Ages are given as median probability with error bars representing 2σ ranges of pre-bomb calibration, except for the uppermost radiocarbon date which is given as 2σ range mean of post-bomb calibration, error in size of the symbol. Two dates had to be rejected as they are likely to contain reworked 'old' carbon.

4.3. Physical properties and mineralogy

The water content (WC) shows a general increasing trend from the base (77%) towards the top (85%) of the core. The positive anomaly of 87% around AD 1740 is preceded by a zone of markedly lower values in the second half of the 17th century. The maximum in the mid-18th century corresponds to the transition between lithological units B and C (Fig. 5). In contrast, dry density (DD) exhibits an opposite trend with higher values near the base (0.24 g cm^{-3}) to lower values at the top (0.14 g cm^{-3}) (Fig. 5). Volume specific magnetic susceptibility (κ) is characterized by rising values from the base ($340 \cdot 10^{-6}$ SI) to the maximum of the whole record ($560 \cdot 10^{-6}$ SI) at AD 1240 in lithological unit B. This increase is interrupted by a local minimum ($270 \cdot 10^{-6}$ SI) in lithological unit A around AD 560. After AD 1240 values are decreasing again towards the top of the core ($120 \cdot 10^{-6}$ SI) with a marked positive anomaly between AD 1680 and AD 1730 and an excursion to lower values in the second half of the 18th century, both being separated by a marked change at the transition between lithological units B and C (Fig. 5). X-ray diffraction (XRD) analyses revealed the presence of plagioclase, augite, quartz and biogenic opal in all samples. In addition, vivianite was detected in the samples of lithological unit B.

4.4. Stable isotopes

The record of $\delta^{13}C_{org}$ (Fig. 5) is characterized by comparatively high values for lacustrine organic matter, ranging between −18.4 and −21.0‰. The rising and subsequently declining values in lithological unit A reach the least negative values in the 6th century, followed by a relatively stable period with more negative values (mean: −20.3‰) in lithological unit B. Positive excursions are found in the 15th century

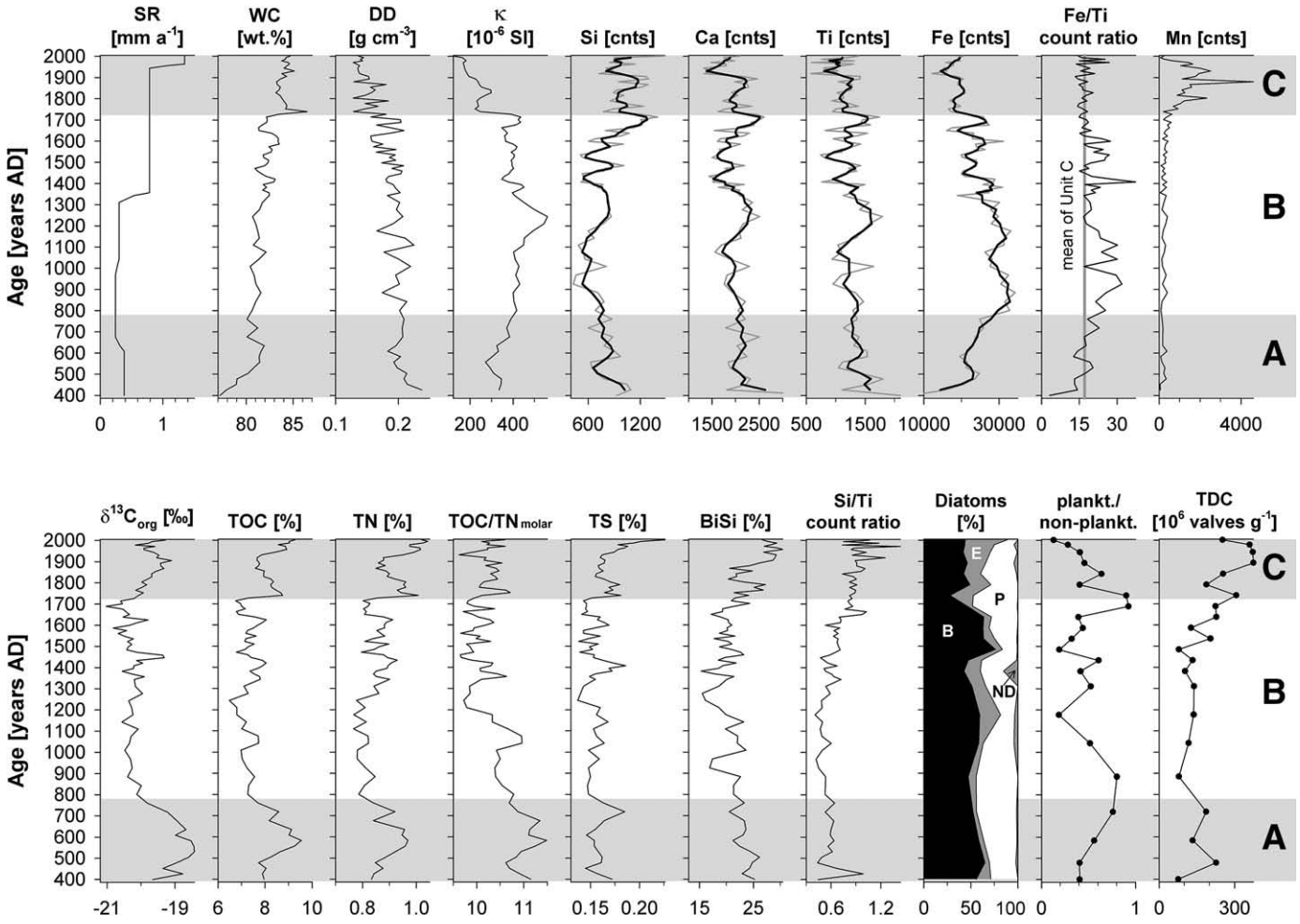

Fig. 5. Multi-proxy data of the core VIZ 05/6 from Laguna Las Vizcachas. SR: sedimentation rate, WC: water content, DD: dry density, κ: volume specific magnetic susceptibility, TOC: total organic carbon, TN: total nitrogen, TS: total sulfur, BiSi: biogenic silica, Diatoms (B: benthic taxa, E: epiphytic taxa, P: planktonic taxa, ND: no data), plankt./non-plankt.: %-ratio planktonic/non-planktonic diatoms, TDC: total diatom concentration. XRF-data of the elements Si, Ca, Ti, Fe and Mn are given in total counts [cnts], gray line: original data, bold line: 3 point running mean. Horizontal gray and white bars refer to the lithological units A, B and C.

and the first half of the 17th century. In lithological unit C, values are rising markedly reaching a local maximum of −19.1‰ around AD 1900. Afterwards values become more negative again but increase during the last decades of the 20th century.

4.5. Geochemistry

Among the elements determined by XRF-scanning only Si, Ca, Ti, Fe and Mn are reported here (Fig. 5). Other elements either provide the same type of information (e.g., Al, K) or exhibit counting rates that are too low for a reliable interpretation. The elements Si, Ca and Ti all show a similar high-frequency pattern and are significantly (p value < 0.01) correlated with each other: Spearman–Rho correlation coefficients (r_s) are 0.44 (Si vs. Ti), 0.85 (Ca vs. Ti) and 0.61 (Si vs. Ca). Most characteristic in the patterns of Si, Ca and Ti is a zone of comparatively high values from AD 1150 until AD 1400 with a peak in the 13th century. Unlike in other parts of the record this zone is characterized by the absence of any significant excursion to low values. After some fluctuations to lower values in the 15th and 16th century there is an increase of Si, Ca and Ti in the 17th century until a maximum is reached around AD 1700, followed by a decline at the transition between lithological units B and C (beginning of the 18th century). Finally, there is a rise in the 19th century peaking around AD 1900 followed by a sharp decline and subsequently rising values. Superimposed on this high-frequency pattern, only Si exhibits a slightly increasing long-term trend towards the top starting in the upper part of lithological unit B. This trend is also reflected by the Si/Ti total counts ratio (Fig. 5). Fe features a partly different pattern (e.g., Fe vs. Ti: $r_s = 0.34$). In lithological unit A, Fe shows an increase from the base until the transition to lithological unit B (ca. AD 780) interrupted by a reversal to a local minimum around AD 580. Shortly after the transition to lithological unit B, Fe reaches the absolute maximum with values exceeding 34,000 cnts. Subsequently, Fe shows a general declining trend largely following the high-frequency pattern of Si, Ca and Ti in the uppermost part of lithological unit B and in lithological unit C. The Fe/Ti total counts ratio (Fig. 5) exhibits an increasing trend in lithological unit A which continues into the lower part of lithological unit B where a maximum is reached. Further above there are strong fluctuations between high and intermediate values, whereas Fe/Ti counts ratios remain stable in the uppermost part of lithological unit B and in unit C. With respect to the mean of lithological unit C, Fe/Ti counts ratios in lithological unit B are either higher or similar to the mean, while in lithological unit A values are lower. Mn is characterized by a totally different pattern with low values (mean: 250 cnts) in lithological units A and B, followed by a pronounced increase up to 4600 cnts in the middle of lithological unit C and a subsequent steep decline to low values towards the top of the core.

TOC, TN, TS and BiSi are all significantly (p value < 0.01) correlated with each other. TOC exhibits a characteristic pattern (Fig. 5) with maxima (>9%) in lithological units A and C while lithological unit B is characterized by lower values around a mean of 7.3%. In lithological

unit A, values are rising from the base towards a maximum from the second half of the 6th until the first half of the 7th century. Thereafter, TOC shows a general declining trend towards the lowest values of the record in the 13th century followed by a general positive trend towards the top of the core. These general trends are interrupted by a local maximum in the 11th century and three local minima from the second half of the 15th century until the first half of the 16th century, from the second half of the 17th century until the beginning of the 18th century, and in the 19th century. The prominent shift towards much higher values in the mid-18th century coincides with the transition to lithological unit C. Subsequently, values are declining again until a further rise in the 20th century. TN follows the same pattern as TOC ($r_s = 0.87$) fluctuating around a mean of 0.9% (Fig. 5). The same is valid for TS (mean: 0.2%), although the correlation with TOC ($r_s = 0.67$) is slightly weaker. In contrast to TOC, the local maximum of TS in lithological unit A is shifted towards the top of the core. It occurs around AD 700. Additionally, TS exhibits no prominent local maximum in the 11th century (Fig. 5). BiSi exhibits values between 15 and 30% (Fig. 5) with a general negative trend from the base towards a minimum in the 13th century and a subsequent positive trend towards the top. Both trends are interrupted by local minima during the 10th and 19th centuries (BiSi vs. TOC: $r_s = 0.59$). The molar ratio of TOC and TN (mean: 10.3) also shows a general decrease from the base towards a minimum in the 13th century; highest values up to 11.5 occur from the second half of the 6th century until the end of the 7th century. This trend is interrupted by a local minimum in the second half of the 5th century and a prominent excursion to higher values in the 11th and 12th centuries. From AD 1300 TOC/TN fluctuates around a mean of 10.1 partly reflecting the pattern of TOC ($r_s = 0.50$, p value < 0.01) (Fig. 5). TIC exhibits values below the detection limit suggesting the absence of carbonates throughout the entire record.

4.6. Diatoms

The diatom flora of the record is dominated by the two planktonic species *Aulacoseira distans* (mean: 19.6%) and *Discostella stelligera* (mean: 9.3%) as well as by a group of small, fragilarioid, benthic taxa (mean: 43.4%) consisting of *Staurosira construens* var. *venter* (dominant), *Staurosirella pinnata*, *Pseudostaurosira brevistriata* and *Staurosira* cf. *laucensis*. 14 additional taxa exhibit relative abundances of at least 3% in at least one sample, i.e., planktonic *Aulacoseira tethera* and the epiphytics *Cocconeis placentula* var. *euglypta*, *Epithemia adnata* and *Gomphonema* spp. as well as the benthics *Achnanthidium minutissimum, Encyonema minutum*, *Encyonema silesiacum*, *Fragilaria capucina*, *Fragilaria* sp. and *Karayevia clevei*. All results are presented and discussed using summarizing taxa groups according to their life forms (benthic, epiphytic, planktonic). The record (Fig. 5) is characterized by a high abundance of benthic taxa (mean: 52%) followed by planktonic (mean: 31%) and epiphytic (mean: 15%) taxa. The percentage ratio of planktonic and non-planktonic taxa fluctuates around a mean of 0.48. From the base until the beginning of the 15th century benthic taxa remain comparatively stable. A steep rise in the mid-15th century marks a change towards highest values (max. 76%) lasting until the mid-17th century. Subsequently, a stable period on a slightly lower level than prior to AD 1400 continues until the top, only interrupted by a negative excursion in the mid-18th century. Epiphytic taxa exhibit extremely low values (mean: 8%) from the base until around AD 1700 interrupted by a period of slightly higher values from the 12th until the mid-15th century. A conspicuous rise in the mid-18th century, corresponding to the transition between lithological units B and C, leads to a period with highest values culminating close to the top (45%). The distribution of planktonic taxa coincides with the planktonic/non-planktonic ratio (Fig. 5) and shows an increase in the 6th century culminating in the 8th and 9th century and a subsequent decline to a local minimum in the second half of the 12th century. Afterwards, values fluctuate with a local maximum from the 14th until the mid-15th century immediately followed by a local minimum. Between the end of the 17th and the mid-18th century a marked shift to highest values occurs (48%, ratio 0.92), which is followed by a decline starting shortly above the transition between lithological units B and C. The lowest values of planktonic taxa and lowest planktonic/non-planktonic ratios of the entire record (11%, ratio 0.13) are found close to the top. Total diatom concentration (mean: 195 million valves g^{-1}) exhibits slightly elevated values in lithological unit A followed by low values in lithological unit B until around AD 1500. From the mid-16th century onwards, values are rising until highest values are reached in the late 19th and in the 20th century (Fig. 5).

5. Discussion

5.1. Sediment accumulation, clastic input and early diagenesis

Sedimentation rates (SR) exhibit a step-like character (Fig. 5) which is a result of linear interpolation between the data points used for the age–depth model (Fig. 4). The 'true' SR changes are likely to have taken place more gradually and possibly to a certain degree earlier or later. However, the general trend of SR changes can be considered as realistic; hence lower SR until the 13th century and higher SR thereafter have to be considered for further interpretation. A higher SR may be the result of either increased minerogenic input, higher productivity in the lake and/or enhanced organic matter preservation. While the general trends of water content (WC) and dry density (DD) most likely reflect increasing compaction with depth, high-frequency variations are assumed to reflect different changing proportions of minerogenic and organogenic components (Fig. 5). Hence, lower WC and higher DD values in the second half of the 17th century indicate enhanced input of clastic material while the positive excursion of WC after the transition from lithological unit B to C is caused by a layer of macrophyte remains. The latter are likely to have been transported towards the coring location by wind-induced water movement. As discussed in the following sections, these macrophyte remains may have come from near-shore or may point to macrophytes growing close to the center of the lake. The patterns of Si, Ca and Ti are very similar (Fig. 5) and are expected to be controlled by the same process. This process is assumed to reflect minerogenic input as inferred from the immobile element Ti which has been used as an indicator for clastic input in other studies (Haug et al., 2003; Demory et al., 2005; Haberzettl et al., 2005, 2007). Due to Ca bearing volcanic rocks in the catchment (plagioclase was detected by XRD analyses) and the absence of any autochthonous carbonates (TIC is below detection limit), Ca matches the pattern of Ti very well. Si shows a mixed signal of allochthonous clastic input (high-frequency pattern) and autochthonous production of biogenic silica (BiSi) mainly by diatoms (long-term trends). This is supported by the comparison between the records of Si, Ti and BiSi (Fig. 5). Although Fe broadly follows the high-frequency pattern of Ti and Ca in parts of lithological unit B and in unit C (Fig. 5), there is evidence for some early diagenetic overprint superimposed on the pattern derived from clastic input. This is supported by a pronounced Mn enrichment in lithological unit C which gives clear evidence for diagenetic Mn precipitation within a depth range slightly above the Fe-redox boundary (Froelich et al., 1979; Kasten et al., 2003) (Fig. 5). Consequently, higher Fe values in lithological unit B and the positive trend with depth may be interpreted analogously as diagenetic enrichment commonly taking place along the Fe(II)/Fe(III) redox boundary (Kasten et al., 2003). This is supported by the presence of the secondary Fe-mineral vivianite (Fagel et al., 2005) as detected by XRD analyses. The distinctly lower Fe values in lithological unit A (Fig. 5) are probably the result of reductive Fe dissolution below the redox boundary (Kasten et al., 2003). Fe dissolution and precipitation in lithological units A and B is also reflected in the Fe/Ti total counts ratios (Fig. 5) with low

values in lithological unit A and high values in lithological unit B, both with respect to the values of lithological unit C. Values in unit C remain comparatively stable and most likely reflect the pre-diagenetic element counts ratio within the clastic material. Hence, Fe/Ti counts ratio excursions above the mean of lithological unit C (Fig. 5) reflect horizons of Fe precipitation while excursions below that mean may indicate Fe dissolution. Magnetic susceptibility (κ) exhibits a pattern similar to Fe ($r_s = 0.80$, p value<0.01) (Fig. 5) suggesting the same controlling factors, i.e., a combined signal of clastic input (Sandgren and Snowball, 2001) and an early diagenetic overprint. The signal of clastic input is especially obvious around AD 1700 with high κ, Fe and Ti values indicating enhanced input of clastic material, followed by a conspicuous shift to lower values at the transition between lithological units B and C. Both features are also observed in various other parameters (e.g., WC, DD). Diagenetic overprint is reflected by lower values of κ in lithological unit A as a result of dissolution of magnetic Fe minerals. While highest values of κ in the 13th century correspond well with the Ti record, highest values of Fe and Fe/Ti counts ratios in the lower part of lithological unit B precede the peak of κ. This supports post-depositional redistribution of Fe and the precipitation of Fe phases that exhibit no strong magnetic signal. Hence, precipitation horizons visible as positive excursions in the Fe/Ti total counts ratio record are not reflected in the κ record.

5.2. Organic matter — sources, productivity, dilution and preservation

The molar TOC/TN ratios, fluctuating around a mean of 10.3 (Fig. 5) suggest predominantly algal origin of the organic matter. However, these values are at the upper limit of the range commonly attributed to algal organic matter (between 4 and 10, Meyers and Teranes, 2001). This is most likely due to different amounts of admixed aquatic macrophyte debris. This is plausible, as a maximum water depth of 19 m and transparent water due to oligotrophic conditions provide large habitats for macrophyte growth. Although macroscopic remains of macrophytes had been picked out before measuring TOC and TN, microscopic debris may have affected the TOC/TN ratio. The interpretation is confirmed by comparing mean values of TOC/TN and $\delta^{13}C_{org}$ from Laguna Las Vizcachas with typical values for organic matter sources as determined for Laguna Azul and its catchment (Fig. 1) in southern Patagonia (Mayr et al., 2005): the sources for organic matter are algae, littoral sediments, aquatic macrophytes, terrestrial plants and soil organic matter. In this context the values of Laguna Las Vizcachas fit well into the range found in littoral sediments (Mayr et al., 2005). However, minor admixtures of terrestrial plant material cannot be totally excluded. The proportion of soil organic matter is difficult to asses as typical steppe soils from southern Patagonia exhibit values similar to those of algal organic matter with TOC/TN ratios being only slightly higher (Mayr et al., 2005). Assuming that TOC/TN reflects different amounts of macrophyte debris admixed to algal organic matter, highest contributions of macrophytes from the second half of the 6th until the end of the 7th century and in the 11th and 12th century are implied (Fig. 5). This would be in disagreement with low proportions of epiphytic diatom taxa during these periods (Fig. 5) if there were a direct correlation between the abundance of macrophytes and epiphytic diatoms. However, as discussed in the following section, the contribution of epiphytic diatoms to the sediment in the lake center might be strongly controlled by wind-induced lateral water movements rather than by macrophyte growth close to the coring location. Another possible explanation for the pretended disagreement between comparatively high TOC/TN ratios and low proportions of epiphytic diatoms in this section of the record is that, for some unknown synecological reasons, non-diatom algae dominated the epiphytic habitat during these periods. This would have led to low proportions of epiphytic diatoms even though macrophytes were abundant. However, admixtures of soil organic matter or minor amounts of terrestrial plants may have influenced TOC/TN ratios as well. Furthermore, the contribution of biomass from cyanobacteria may also increase TOC/TN ratios (Mayr et al., 2009). Therefore, comparatively high TOC/TN ratios in the lower part of the record are not necessarily to be attributed to higher proportions of macrophyte debris, although this is likely to be the most relevant factor. As TOC, TN, TS and BiSi display a rather similar pattern in Laguna Las Vizcachas (Fig. 5), they are likely to reflect the same controlling factors. These are primary productivity, dilution by minerogenic input, and organic matter preservation as commonly assumed for TOC (Meyers, 2003). BiSi gives evidence confined to silicifying organisms, mainly diatoms. This is confirmed by the record of total diatom concentration (Fig. 5). Autochthonous production of biogenic silica is also reflected by the Si/Ti total counts ratio (Fig. 5) which exhibits similarities to the BiSi record. Both show slightly negative long-term trends from the 5th century until the 12th and 13th century, respectively, which are followed by positive trends towards the top of the record. Superimposed on these general trends BiSi exhibits a high-frequency pattern resulting from dilution by minerogenic material. In contrast, the Si/Ti total counts ratio is independent of these dilution effects whereas total counts of Si and Ti are dependent on the varying intensity of clastic input, which leads to the high-frequency pattern of both elements. The ratio of Si and Ti counts, however, does not show this pattern. Enhanced Si/Ti count ratios might be provoked by eolian input of Si-rich minerogenic material from outside the catchment. Another explanation for elevated Si/Ti count ratios would be the input of Si from biogenic silica. The good agreement between the long-term trends of the Si/Ti ratio and BiSi suggests that these trends are controlled by biogenic silica production rather than eolian input of minerogenic Si. Hence, the Si/Ti total counts ratio may represent the most reliable proxy for the 'true' diatom productivity as it is independent of dilution effects. $\delta^{13}C_{org}$ may constitute another measure of productivity (Meyers, 2003). Thereby, this proxy should be more robust with respect to dilution and re-mineralization than TOC, because it is independent of concentration effects. Hence, comparing the records of TOC and $\delta^{13}C_{org}$ might help to distinguish signals of productivity from those originating from dilution and preservation. However, this line of argument does not apply to the record of Laguna Las Vizcachas where it is likely that $\delta^{13}C_{org}$ (Fig. 5) is rather controlled by varying contributions of different organic matter sources, i.e., admixtures of algal organic matter and macrophyte debris. Albeit macroscopic remains had been eliminated by the sieving procedure prior to the isotopic measurements, microscopic macrophyte debris <200 µm may affect $\delta^{13}C_{org}$ values. An enhanced contribution of macrophyte debris is obvious at least for lithological unit A where a good agreement between $\delta^{13}C_{org}$ and TOC/TN corroborates the view that the origin of organic matter controls $\delta^{13}C_{org}$ values. In the two other lithological units there might be some additional influence of productivity interfering with the signal of organic matter sources, which leads to a mixed signal. In light of this ambiguity with $\delta^{13}C_{org}$, the Si/Ti total counts ratio remains the most reliable proxy for 'true' productivity independent of dilution effects. Although being confined to diatom productivity, the increasing trend of Si/Ti from the 13th century towards the top of the core is similarly reflected by the general trends of TOC, TN and TS. Hence, total productivity as reflected in the bulk organic component of the sediment follows the same trend. In contrast, in the lower part of the record the Si/Ti total counts ratio provides only limited information about total productivity, because comparatively low values suggest a minor contribution of diatoms to the total productivity. At the same time macrophyte debris might have contributed significantly to the bulk organic components. Nevertheless, the long-term trends of TOC, TN, TS and BiSi evidence decreasing proportions of organogenic matter from the base of the core until the 13th century followed by increasing proportions towards the top of the core. The resulting opposite long-term trends of the minerogenic fraction are reflected by the significant negative correlation between TOC and κ ($r_s = -0.79$, p value<0.01). In contrast, the correlation between TOC and Ti ($r_s = -0.22$, p value<0.05) is much weaker. Considering that TOC as well as TN, TS

and BiSi are given in weight-%, this difference indicates that κ values are much more affected by dilution effects than element counts obtained by XRF-scanning. As a consequence, the signal of varying intensity of clastic input as inferred from Ca and Ti is not significantly affected by the long-term trends of the organogenic fraction. The high-frequency fluctuations, however, are reflected by opposite patterns in both, Ti and TOC. Hence, this high-frequency pattern gives evidence about the 'true' intensity changes of clastic input as inferred from Ti, while the complementary pattern in TOC is a result of dilution. This is conclusive, because the Ti counts are not affected by the most pronounced increases of TOC weight-% in lithological units A and C, while TOC, nevertheless, reflects the high-frequency variations of Ti. As a result, variations visible in both Ti and TOC are likely to represent changes in clastic input, while changes in productivity or organic matter preservation are likely to be reflected in the TOC record only. The latter is represented by the long-term trends of TOC leading to highest values in lithological units A and C. Changes in productivity may be controlled either by a varying influx of nutrients through fluvial and/or eolian input or the duration of open water or ice cover without snow on the ice, which enables photosynthesis and, hence, controls the length of the growing season for algae and macrophytes.

Variations in the amount and seasonality of precipitation (summer vs. winter) and the duration of winter ice cover are the likely climatic factors controlling the clastic input to the lake and, hence, the high-frequency fluctuations within the Ti and TOC records. Winter ice cover may play an important role regarding sediment formation as Laguna Las Vizcachas is a mountain lake and ice-covered for several months of the year. On the one hand periods of prolonged ice cover on the lake and snow cover in the catchment area reduce the annual duration of fluvial activity and potentially diminish the clastic input to the lake. In addition, organic matter oxidation may be reduced due to longer periods with lake water stratification under ice cover and prolonged anoxic conditions at the sediment/water interface. This leads to higher TOC values. On the other hand longer periods of snow and ice cover may extend the time of snow accumulation in the catchment, hence leading to stronger runoff during the period of snowmelt. This in turn would result in enhanced minerogenic flux to the lake sediments. The duration of winter ice cover is likely controlled by the timing of freezing and melting, and by minimum temperatures in winter which controls the thickness of the ice cover (Livingstone, 2005). Also the amount of winter precipitation and snow accumulation on the ice may affect the duration of winter ice cover as demonstrated for an alpine lake in Switzerland (Lotter and Bigler, 2000). However, the latter factor is probably less relevant at Laguna Las Vizcachas, because precipitation is much lower than in the Alps (Ohlendorf et al., 2000).

5.3. Diatoms

The diatom record points to continuously oligotrophic conditions as indicated, for example, by the two dominant planktonic species *Aulacoseira distans* and *Discostella stelligera* (De Wolf, 1982; Urrutia et al., 2000). There is a high abundance of small benthic taxa throughout the entire record (Fig. 5). This reflects very likely the *in situ* situation at the coring location at 16 m water depth where, due to the oligotrophic conditions, good light penetration permits the development of an abundant and diverse benthic diatom flora. In addition, the comparatively long duration of winter ice cover favors benthic and epiphytic diatoms over planktonic taxa: non-planktonic species continue photosynthesis underneath the ice in early winter as long as there is no snow on the ice while planktonic species sink to the ground due to the lack of turbulence (Lotter and Bigler, 2000). Furthermore, non-planktonic species are favored at the end of the winter as the ice commonly starts melting from the shore towards the center of the lake. This enables light penetration first in the littoral habitat from where non-planktonic diatoms are transported to the coring location by lateral water movement while the ice cover on the lake center still restricts planktonic diatom growth (Lotter and Bigler, 2000). Thus, non-planktonic diatoms are also the first to use the nutrients which may have been mobilized from the sediments during winter stratification. This might constitute an important competitive advantage within an oligotrophic lake ecosystem. The ratio of planktonic to non-planktonic diatom taxa has been used as an indicator for the length or presence/absence of winter ice cover in alpine and arctic environments (Lotter and Bigler, 2000; Lotter et al., 2000; Ohlendorf et al., 2000; Cremer et al., 2001), and high proportions of benthic fragilarioid taxa have been related to cold conditions (Stoermer, 1993 and references therein). Applying this model to Laguna Las Vizcachas points to an extended length of the ice cover from the mid-15th until the mid-17th century when coldest conditions are inferred from higher proportions of benthic taxa (mainly the small benthic fragilarioids; Fig. 5). This period is followed by an increase of planktonic taxa with highest planktonic/non-planktonic ratios around the transition between lithological units B and C (Fig. 5), which points to reduced ice cover and warmer conditions. Similarly, higher proportions of planktonic diatoms suggest also warmer conditions culminating in the 8th and 9th century (Fig. 5). Higher proportions of epiphytic taxa from the 12th until the mid-15th century and increasing values from the 18th century onwards (Fig. 5) might be interpreted in terms of good conditions for macrophyte growth. This may be the result of increased availability of nutrients or enhanced light transmission in the water column and expansion of the macrophyte habitat towards the lake center. Indeed, from the 18th century until the top of the core (i.e., lithological unit C), higher proportions of epiphytic taxa correspond to layers with macrophyte remains (Fig. 3). In contrast, the sediments with enhanced proportions of epiphytic taxa from the 12th until the mid-15th century do not show macroscopic macrophyte remains and point to an alternative interpretation for that period within lithological unit B which may also apply (alternatively or additionally) to lithological unit C. Higher proportions of epiphytic taxa seem to occur at the expense of planktonic taxa while benthic taxa remain comparatively stable during both periods (Fig. 5). We suggest that higher proportions of epiphytic taxa point to stronger wind-induced lateral water movements and thus to enhanced transport of epiphytic diatoms from macrophytes in the littoral habitat towards the center of the lake (coring position) where they are sedimented from the water column together with planktonic diatoms. Turbulent water movements would predominantly mobilize epiphytic diatoms while benthic diatoms would be less affected. Hence, the occurrence of benthic taxa in the record can be considered as *in situ*, while the abundance of epiphytic taxa might give information about wind intensities. Following this line of argument, the layers of macrophyte remains in lithological unit C may also be interpreted in terms of strongest wave action which displaced macrophytes towards the coring location. This is consistent with highest proportions of epiphytic diatoms in that section of the sediments.

5.4. Palaeoenvironmental inferences

A synopsis of the various lines of interpretation for the different parameters results in the following most probable scenario of the palaeoenvironmental history (Fig. 6):

High values of TOC from the 6th until the first half of the 8th century point to comparatively high productivity and/or good organic matter preservation. In addition, higher values of TOC/TN and $\delta^{13}C_{org}$ may point to higher proportions of admixed macrophyte debris. The climatic forcing factor remains unclear as neither Ti nor the planktonic/non-planktonic diatom ratio provide unambiguous climate signals. Ti provides no evidence of increased supply of nutrients through enhanced fluvial and/or eolian input. The planktonic/non-planktonic diatom ratio is not in phase with TOC. Hence, evidence is

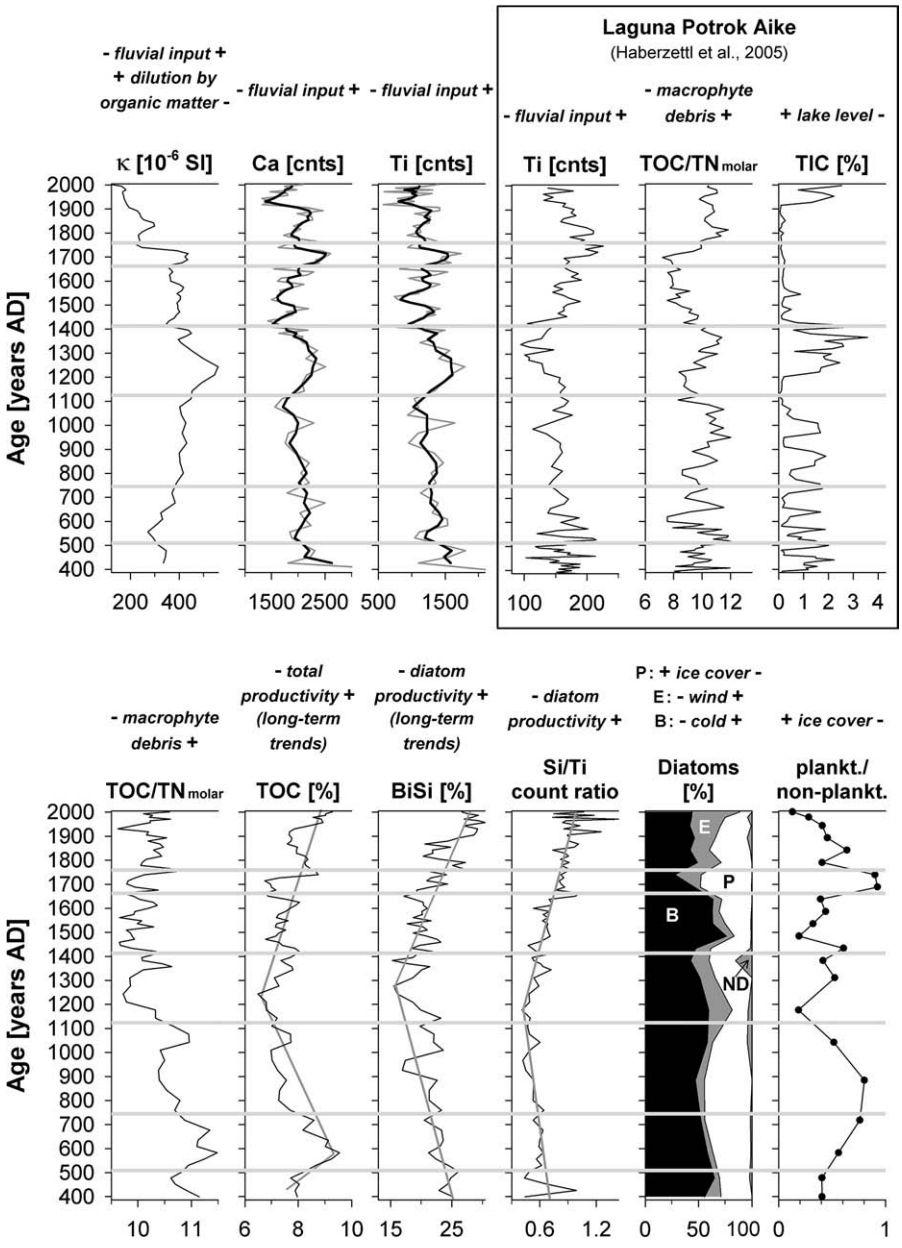

Fig. 6. Selected parameters from Laguna Las Vizcachas (this study) and Laguna Potrok Aike (Haberzettl et al., 2005) with palaeoenvironmental inferences. For abbreviations see Fig. 5, TIC: total inorganic carbon. Straight lines in TOC, BiSi and Si/Ti count ratio refer to long-term trends. Gray bars separate distinct periods discussed in the text.

not unambiguous, neither for higher productivity as a result of reduced ice cover nor for enhanced organic matter preservation as a result of prolonged ice cover. From the 12th until the end of the 14th century Ti, Ca and κ provide a much clearer climatic signal of a period with constantly enhanced clastic input (Fig. 6). As Laguna Las Vizcachas has an inflow, fluvial rather than eolian origin is likely for the clastic input. As the planktonic/non-planktonic diatom ratio is not in phase with this period we conclude that the duration of ice cover is not a major factor controlling the intensity of clastic input. In contrast, the amount of precipitation is likely to be much more important. A higher contribution of epiphytic diatoms during the same period points to stronger wind-induced lateral water movements and, hence, suggests stronger wind intensities at times with higher precipitation. This period of sustained enhanced clastic input due to higher precipitation coincides partly with the 'Medieval Climate Anomaly' (MCA) as registered in the lake sediments of Laguna Potrok Aike (Figs. 1, 6), a maar lake in lowland south-eastern Patagonia about 175 km SE of Laguna Las Vizcachas (Haberzettl et al., 2005). However, there is a disagreement with the climatic inferences of Haberzettl et al. (2005) who report dry conditions and low lake levels at Laguna Potrok Aike during this period. This discrepancy might be an artifact due to inherent uncertainties of the age–depth models of both records. However, the age–depth models of both lakes are relatively reliable during the period under consideration (Fig. 4, Haberzettl et al., 2005). Therefore, we hypothesize that precipitation regimes at both locations were inverse. At Laguna Potrok Aike, dry conditions were attributed to stronger westerly wind intensities weakening the influence of south-easterly winds. This is fundamental for the hydrological balance as the easterly winds are an important source of moisture in lowland south–eastern Patagonia (Mayr et al., 2007b). However, at Laguna Las Vizcachas, located further to the west and much closer to the Andes, easterly winds would not be significant as they loose most of the moisture on the way from the Atlantic Ocean across the Patagonian mainland. In contrast, we hypothesize that enhanced westerly winds

lead to higher precipitation at Laguna Las Vizcachas. At the same time an increased foehn effect and drier conditions due to higher westerly wind velocities may become effective only at lower elevations and further to the east. While direct meteorological data for Laguna Las Vizcachas are not available to test this hypothesis, investigations in southern Chile (Schneider et al., 2003) support our hypothesis: observations across the southern Andes at 53°S reveal that the Gran Campo Nevado area (Fig. 1; close to the main divide of the Andes) obtains most of the rain from strong westerly air flows, while other synoptic patterns govern the water balance at Punta Arenas (Fig. 1; located in the steppes east of the Andes) (Schneider et al., 2003). The northern shore of Seno Skyring (Fig. 1; at the eastern foot of the Andes; the most likely analog to Laguna Las Vizcachas) exhibits a situation similar to the Gran Campo Nevado, but foehn conditions are frequent and precipitation amounts are lower. The most pronounced foehn conditions occur at Punta Arenas (Schneider et al., 2003). In comparison with Seno Skyring, Laguna Las Vizcachas is expected to experience weaker foehn conditions which would result in enhanced precipitation with stronger westerly winds. While the data from Seno Skyring were derived from near sea level, the high elevation of Laguna Las Vizcachas restricts adiabatic warming of the sinking air, particularly in the catchment area on Meseta de las Vizcachas at about 1400 m a.s.l.

The hypothesis of inverse precipitation regimes between the western and the eastern parts of southern Patagonia during Medieval times is challenged by evidence of dry climatic conditions in locations at longitudes comparable to Laguna Las Vizcachas. Radiocarbon dating of relict tree stumps rooted in present-day lakes and marshes indicates a Medieval lake level low stand for Lago Cardiel (48°57′S, 71°26′W; Fig. 1) and drier conditions at Catalon Marsh in the Lago Argentino area (50°28′S, 72°58′W; Fig. 1) (Stine, 1994). Dry conditions allowed trees to grow at these sites while the death of the trees has been related to rising lake and water table levels. Tree death has been determined to the range of AD 1021–1228 for Lago Cardiel and AD 1051–1226 for Catalon Marsh (1σ range of calibration) (Stine, 1994). These dates might dismiss or support the hypothesis of inverse precipitation regimes depending on the dating errors allowed for all archives under comparison. However, it is more likely that the dry conditions as found in Lago Cardiel and in Catalon Marsh preceded the period of higher precipitation inferred from the record of Laguna Las Vizcachas, where the wet period is ascribed to the time from the 12th until the end of the 14th century. Thus, the beginning of the increasingly wet conditions might coincide in the three areas. As a consequence, for the western parts of southern Patagonia east of the Andes, consistent evidence from Lago Cardiel, Catalon Marsh and Laguna Las Vizcachas suggests comparatively dry conditions during earlier Medieval times followed by comparatively wet conditions during late Medieval times. This might corroborate the hypothesis of inverse precipitation regimes between the western and the eastern parts of southern Patagonia as the record of Laguna Potrok Aike in the east (Fig. 1) suggests an inverse situation: wet conditions with a high lake level prevailed during the 12th century and dry conditions with low lake levels during the 13th and 14th century (Haberzettl et al., 2005) (Fig. 6). However, these inferences are subject to the age uncertainties of all records considered.

After the late Medieval period with high precipitation and, hence, increased fluvial runoff, the record of Laguna Las Vizcachas shows a prominent shift towards colder conditions as indicated by highest proportions of benthic diatom taxa. Cold conditions culminated between the mid-15th and the mid-17th century (Fig. 6), which coincides with the beginning of the 'Little Ice Age' (LIA). This is consistent with the record of Laguna Potrok Aike (Figs. 1, 6) where a more positive water balance due to higher precipitation (inferred from the Ti record) and possibly also colder temperatures caused a significant lake level rise (Haberzettl et al., 2005). At Laguna Las Vizcachas, the cold period ends around the mid-17th century, when a conspicuous rise of the planktonic/non-planktonic diatom ratio and a relative decrease in benthic taxa (Fig. 6) point to shorter winter ice cover (and hence better growing conditions for planktonic diatoms) related to warmer or shorter winters or less snow cover on the ice. At the same time, proxies indicate stronger fluvial input to the lake as a result of higher precipitation and/or of longer annual duration of fluvial activity, i.e., a shorter time in winter without running water. This period lasts until the mid-18th century when many proxies show prominent shifts (transition between lithological units B and C, Fig. 5). These shifts coincide with changes in the record of Laguna Potrok Aike (Figs. 1, 6) (Haberzettl et al., 2005), where a conspicuous rise of TOC/TN and a change from increasing to decreasing trends of Ti point to the onset of decreasing precipitation and mobilization of littoral macrophyte organic matter during the incipient lake level regression. In the record of Laguna Las Vizcachas the shift towards lower values of Ti and κ in the mid-18th century points to reduced fluvial activity followed by a slight increase in the 19th century (Fig. 6). The same interpretation may apply for another shift towards lower values that occurred around AD 1900 followed by a subsequent increase in the 20th century (Fig. 6; most obvious in the record of Ca due to its higher element counts). However, this uppermost part of the record has to be interpreted with caution as during the late 19th and 20th century human impact is possible, but difficult to assess and difficult to distinguish from climatic signals. Higher proportions of epiphytic diatoms from the mid-18th century until the top of the core point to increased wind intensities and/or better conditions for macrophyte growth. The long-term trends of TOC, BiSi and Si/Ti total counts ratio which increase from the 13th century until the top of the record (Fig. 6) evidence increasing productivity. The forcing factor, however, remains unclear.

6. Conclusions

Climatic interpretations based on data from Laguna Las Vizcachas compared with other records provide information about climatic changes during the last millennium, give evidence about their regional extent, and contribute to distinguish between the signals of temperature and precipitation. The record evidences a period of enhanced fluvial activity as a result of higher precipitation from the 12th until the end of the 14th century which may coincide with higher wind intensities. Thereby, it might corroborate the timing of the most prominent, younger period of the 'Medieval Climate Anomaly' as postulated for Laguna Potrok Aike (Haberzettl et al., 2005) further to the south-east. We hypothesize inverse precipitation regimes between the western and the eastern parts of extra-Andean southern Patagonia during that time. That means that conditions were comparatively wet at Laguna Las Vizcachas in the west, while Laguna Potrok Aike in the east (Fig. 1) experienced dry conditions. Thus, the record of Laguna Las Vizcachas may contribute to a better understanding of the spatial distribution of past hydrological changes in southern Patagonia. In addition, the presented data from Laguna Las Vizcachas reveal signals of temperature changes as inferred from the diatom record, i.e., coldest conditions of the record from the mid-15th until the mid-17th century, followed by warmest conditions of the last millennium from the mid-17th until the mid-18th century. Hence, these data provide new insights into climatic variability in southern Patagonia within a period corresponding to the 'Little Ice Age' of the northern hemisphere.

Future research should focus on additional testing of the presented hypotheses. Qualitative climatic estimates from pollen analyses, and quantitative reconstructions of precipitation and temperature using pollen transfer functions, may provide additional information on the local and regional scale. Spatial patterns of hydrological changes and their links to large-scale atmospheric circulation might be tested and evaluated by applying regional and downscaled global climate models.

Acknowledgements

The authors would like to express their thanks to the owner of Estancia Las Vizcachas for permitting access to the lake. The staff of INTA, Río Gallegos are acknowledged for their assistance in organizing the logistics of the field work. We thank Sabine Stahl for assistance with sampling and geochemical analyses. We are much obliged to Thomas Frederichs and Christian Hilgenfeldt (Department of Marine Geophysics, University of Bremen) for access to their magnetic susceptibility measuring bench. Stephanie Janssen and Michael Wille are acknowledged for inspiring discussions and excellent collaboration in the SALSA-team. We thank Daniel Ariztegui and an anonymous reviewer for valuable comments on an earlier version of the manuscript. An anonymous language editor is acknowledged for improvements in language and style of the English text. This is a contribution to the project "South Argentinean Lake Sediment Archives and modeling" (SALSA) within the framework of the German Climate Research Program DEKLIM (grants 01 LD 0034 and 0035) of the German Federal Ministry of Education and Research (BMBF). Additional financial support was provided by the German Science Foundation (DFG) in the framework of the Priority Program 'ICDP' (grant ZO 102/5-1, 2, 3).

References

Battarbee, E.W., 1986. Diatom analysis. In: Berglund, B.E. (Ed.), Handbook of Holocene Palaeoecology and Palaeohydrology. J. Wiley & Sons, New York, pp. 527–570.

Cremer, H., Wagner, B., Melles, M., Hubberten, H.-W., 2001. The postglacial environmental development of Raffles Sø, East Greenland: inferences from a 10,000 year diatom record. Journal of Paleolimnology 26, 67–87.

Dearing, J., 1994. Environmental Magnetic Susceptibility: Using the Bartington MS2 System. Chi Publishing, Kenilworth. 104 pp.

Demory, F., Oberhänsli, H., Nowaczyk, N.R., Gottschalk, M., Wirth, R., Naumann, R., 2005. Detrital input and early diagenesis in sediments from Lake Baikal revealed by rock magnetism. Global and Planetary Change 46 (1–4), 145–166.

De Wolf, H., 1982. Method of coding of ecological data from diatoms for computer utilization. Mededelingen Rijks Geologische Dienst. Nieuwe Serie 36 (2), 95–110.

Fagel, N., Alleman, L.Y., Granina, L., Hatert, F., Thamo-Bozso, E., Cloots, R., André, L., 2005. Vivianite formation and distribution in Lake Baikal sediments. Global and Planetary Change 46, 315–336.

Fesq-Martin, M., Friedmann, A., Peters, M., Behrmann, J., Kilian, R., 2004. Late-glacial and Holocene vegetation history of the Magellanic rain forest in southwestern Patagonia, Chile. Vegetation History and Archaeobotany 13, 249–255.

Fowler, J., Cohen, L., Jarvis, P., 1998. Practical Statistics for Field Biology. John Wiley & Sons, Chichester. 259 pp.

Froelich, P.N., Klinkhammer, G.P., Bender, M.L., Luedke, N.A., Heath, G.R., Cullen, D., Dauphin, P., Hammond, D., Hartman, B., Maynard, V., 1979. Early oxidation of organic matter in pelagic sediments of the eastern equatorial Atlantic: suboxic diagenesis. Geochimica et Cosmochimica Acta 43, 1075–1090.

Gilli, A., Anselmetti, F.S., Ariztegui, D., Beres, M., McKenzie, J.A., Markgraf, V., 2005a. Seismic stratigraphy, buried beach ridges and contourite drifts: the Late Quaternary history of the closed Lago Cardiel basin, Argentina (49°S). Sedimentology 52 (1), 1–23.

Gilli, A., Ariztegui, D., Anselmetti, F.S., McKenzie, J.A., Markgraf, V., Hajdas, I., McCulloch, R.D., 2005b. Mid-Holocene strengthening of the Southern Westerlies in South America — sedimentological evidences from Lago Cardiel, Argentina (49°S). Global and Planetary Change 49, 75–93.

Haberzettl, T., Fey, M., Lücke, A., Maidana, N., Mayr, C., Ohlendorf, C., Schäbitz, F., Schleser, G.H., Wille, M., Zolitschka, B., 2005. Climatically induced lake level changes during the last two millennia as reflected in sediments of Laguna Potrok Aike, southern Patagonia (Santa Cruz, Argentina). Journal of Paleolimnology 33 (3), 283–302.

Haberzettl, T., Wille, M., Fey, M., Janssen, S., Lücke, A., Mayr, C., Ohlendorf, C., Schäbitz, F., Schleser, G.H., Zolitschka, B., 2006. Environmental change and fire history of southern Patagonia (Argentina) during the last five centuries. Quaternary International 158 (1), 72–82.

Haberzettl, T., Corbella, H., Fey, M., Janssen, S., Lücke, A., Mayr, C., Ohlendorf, C., Schäbitz, F., Schleser, G.H., Wille, M., Wulf, S., Zolitschka, B., 2007. Late glacial and Holocene wet–dry cycles in southern Patagonia: chronology, sedimentology and geochemistry of a lacustrine record from Laguna Potrok Aike, Argentina. Holocene 17 (3), 297–310.

Haberzettl, T., Kück, B., Wulf, S., Anselmetti, F., Ariztegui, D., Corbella, H., Fey, M., Janssen, S., Lücke, A., Mayr, C., Ohlendorf, C., Schäbitz, F., Schleser, G.H., Wille, M., Zolitschka, B., 2008. Hydrological variability in southeastern Patagonia and explosive volcanic activity in the southern Andean Cordillera during Oxygen Isotope Stage 3 and the Holocene inferred from lake sediments of Laguna Potrok Aike, Argentina. Palaeogeography, Palaeoclimatology, Palaeoecology 259, 213–229.

Haug, G., Gunther, D., Peterson, L., Sigman, D., Hughen, K., Aeschlimann, B., 2003. Climate and the collapse of Maya civilization. Science 299, 1731–1735.

Heusser, C.J., 1993. Late Quaternary Forest–Steppe Contact Zone, Isla Grande de Tierra del Fuego, Subantarctic South America. Quaternary Science Reviews 12, 169–177.

Heusser, C.J., 1995. Three Late Quaternary pollen diagrams from Southern Patagonia and their palaeoecological implications. Palaeogeography, Palaeoclimatology, Palaeoecology 118, 1–24.

Heusser, C.J., 1998. Deglacial paleoclimate of the American sector of the Southern Ocean: Late Glacial–Holocene records from the latitude of Canal Beagle (55°S), Argentine Tierra del Fuego. Palaeogeography, Palaeoclimatology, Palaeoecology 141, 277–301.

Hoffman, J.A.J., 1975. Atlas climatológico de América del Sur. OMM–WMO–UNESCO, Hungría.

Hua, Q., Barbetti, M., 2004. Review of tropospheric bomb 14C data for carbon cycle modeling and age calibration purposes. Radiocarbon 46 (3), 1273–1298.

Huber, U.M., Markgraf, V., 2003. European impact on fire regimes and vegetation dynamics at the steppe–forest ecotone of southern Patagonia. Holocene 13 (4), 567–579.

Huber, U.M., Markgraf, V., Schäbitz, F., 2004. Geographical and temporal trends in Late Quaternary fire histories of Fuego–Patagonia, South America. Quaternary Science Reviews 23, 1079–1097.

Kasten, S., Zabel, M., Heuer, V., Hensen, C., 2003. Processes and signals of nonsteady-state diagenesis in deep-sea sediments and their pore waters. In: Wefer, G., Mulitza, S., Ratmeyer, V. (Eds.), The South Atlantic in the Late Quaternary: Reconstruction of Material Budget and Current Systems. Springer, pp. 431–459.

Kelts, K., Briegel, U., Ghilardi, K., Hsü, K., 1986. The limnogeology–ETH coring system. Schweizerische Zeitschrift Hydrol für Hydrologie 48 (1), 104–115.

Krammer, K., Lange-Bertalot, H., 1986. Bacillariophyceae 1. Teil: Naviculaceae. In: Ettl, H., Gerloff, J., Heynig, H., Mollenhauer, D. (Eds.), Süßwasserflora von Mitteleuropa. G. Fischer, Jena, pp. 1–876.

Krammer, K., Lange-Bertalot, H., 1988. Bacillariophyceae 2. Teil: Bacillariaceae, Epithemiaceae, Surirellaceae. In: Ettl, H., Gerloff, J., Heynig, H., Mollenhauer, D. (Eds.), Süßwasserflora von Mitteleuropa. G. Fischer, Jena, pp. 1–596.

Krammer, K., Lange-Bertalot, H., 1991a. Bacillariophyceae 3. Teil: Centrales, Fragilariaceae, Eunotiaceae. Unter Mitarbeit von H. Håkansson und M. Nörpel. In: Ettl, H., Gerloff, J., Heynig, H., Mollenhauer, D. (Eds.), Süßwasserflora von Mitteleuropa. G. Fischer, Stuttgart, Jena, pp. 1–576.

Krammer, K., Lange-Bertalot, H., 1991b. Bacillariophyceae 4. Teil: Achnanthaceae, Kritische Ergänzungen zu Navicula (Lineolatae) und Gomphonema. In: Ettl, H., Gerloff, J., Heynig, H., Mollenhauer, D. (Eds.), Süßwasserflora von Mitteleuropa. G. Fischer, Stuttgart, Jena, pp. 1–437.

León, R.J.C., Bran, D., Collantes, M., Paruelo, J.M., Soriano, A., 1998. Grandes unidades de vegetación de la Patagonia extra andina. Ecologia Austral 8, 125–144.

Livingstone, D.M., 2005. Ice cover on lakes and rivers. Climate trends inferred from historical records. EAWAG News 58e, 19–22.

Lotter, A.F., Bigler, C., 2000. Do diatoms in the Swiss Alps reflect the length of ice-cover? Aquatic Sciences 62, 125–141.

Lotter, A.F., Hofmann, W., Kamenik, C., Lami, A., Ohlendorf, C., Sturm, M., van der Knaap, W.O., van Leeuwen, J.F.N., 2000. Sedimentological and biostratigraphical analyses of short sediment cores from Hagelseewli (2339 m a.s.l.) in the Swiss Alps. Journal of Limnology 59 (Suppl. 1), 53–64.

Lowe, R.L., 1974. Environmental requirements and pollution tolerance of freshwater diatoms. Report EPA-670/4-74-005, Environmental Protection Agency, Cincinnati, Ohio.

Mancini, M.V., 1998. Vegetational changes during the Holocene in Extra-Andean Patagonia, Santa Cruz Province, Argentina. Palaeogeography, Palaeoclimatology, Palaeoecology 138, 207–219.

Mancini, M.V., Paez, M.M., Prieto, A.R., Stutz, S., Tonello, M., Vilanova, I., 2005. Mid-Holocene climatic variability reconstruction from pollen records (32°–52°S, Argentina). Quaternary International 132, 47–59.

Markgraf, V., Bradbury, J.P., Schwalb, A., Burns, S.J., Stern, C., Ariztegui, D., Gilli, A., Anselmetti, F.S., Stine, S., Maidana, N., 2003. Holocene palaeoclimates of southern Patagonia: limnological and environmental history of Lago Cardiel, Argentina. Holocene 13 (4), 581–591.

Mayr, C., Fey, M., Haberzettl, T., Janssen, S., Lücke, A., Maidana, N.I., Ohlendorf, C., Schäbitz, F., Schleser, G.H., Struck, U., Wille, M., Zolitschka, B., 2005. Palaeoenvironmental changes in southern Patagonia during the last millennium recorded in lake sediments from Laguna Azul (Argentina). Palaeogeography, Palaeoclimatology, Palaeoecology 228, 203–227.

Mayr, C., Lücke, A., Stichler, W., Trimborn, P., Ercolano, B., Oliva, G., Ohlendorf, C., Soto, J., Fey, M., Haberzettl, T., Janssen, S., Schäbitz, F., Schleser, G.H., Wille, M., Zolitschka, B., 2007a. Precipitation origin and evaporation of lakes in semi-arid Patagonia (Argentina) inferred from stable isotopes (d18O, d2H). Journal of Hydrology 334, 53–63.

Mayr, C., Wille, M., Haberzettl, T., Fey, M., Janssen, S., Lücke, A., Ohlendorf, C., Oliva, G., Schäbitz, F., Schleser, G.H., Zolitschka, B., 2007b. Holocene variability of the Southern Hemisphere westerlies in Argentinean Patagonia (52°S). Quaternary Science Reviews 26, 579–584.

Mayr, C., Lücke, A., Maidana, N.I., Wille, M., Haberzettl, T., Corbella, H., Ohlendorf, C., Schäbitz, F., Fey, M., Janssen, S., Zolitschka, B., 2009. Isotopic fingerprints on lacustrine organic matter from Laguna Potrok Aike (southern Patagonia, Argentina) reflect environmental changes during the last 16,000 years. Journal of Paleolimnology 42, 81–102.

McCormac, F., Hogg, A., Blackwell, P., Buck, C., Higham, T., Reimer, P., 2004. SHCal104 Southern Hemisphere Calibration 0–11.0 cal kyr BP. Radiocarbon 46, 1087–1092.

McCulloch, R.D., Davies, S.J., 2001. Late-glacial and Holocene palaeoenvironmental change in the central Strait of Magellan, southern Patagonia. Palaeogeography, Palaeoclimatology, Palaeoecology 173, 143–173.

Meyers, P.A., 2003. Applications of organic geochemistry to paleolimnological reconstructions: a summary of examples from the Laurentian Great Lakes. Organic Geochemistry 34 (2), 261–289.
Meyers, P.A., Teranes, J.L., 2001. Sediment organic matter. In: Last, W.M., Smol, J.P. (Eds.), Tracking Environmental Change Using Lake Sediments. Physical and Geochemical Methods, vol. 2. Kluwer Academic Publishers, Dordrecht, pp. 239–269.
Müller, P.J., Schneider, R., 1993. An automated leaching method for the determination of opal in sediments and particulate matter. Deep-Sea Research 40 (3), 425–444.
Nowaczyk, N.R., 2001. Logging of magnetic susceptibility. In: Last, W.M., Smol, J.P. (Eds.), Tracking Environmental Changes Using Lake Sediments. Basin Analysis, Coring, and Chronological Techniques, vol. 1. Kluwer Academic Publishers, Dordrecht, The Netherlands, pp. 155–170.
Ohlendorf, C., Bigler, C., Goudsmit, G.-H., Lemcke, G., Livingston, D.M., Lotter, A.F., Müller, B., Sturm, M., 2000. Causes and effects of long periods of ice cover on a remote high Alpine lake. Journal of Limnology 59 (Suppl. 1), 65–80.
Oliva, G., González, L., Rial, P., Livraghi, F., 2001. El ambiente en la Patagonia Austral. In: Borrelli, P., Oliva, G. (Eds.), Ganadería ovina sustentable en la Patagonia Austral. INTA Centro Regional Patagonia Sur, Buenos Aires, pp. 19–82.
Paruelo, J.M., Beltrán, A., Jobbágy, E., Sala, O.E., Golluscio, R.A., 1998. The climate of Patagonia: general patterns and controls on biotic processes. Ecologia Austral 8, 85–101.
Prieto, A.R., Stutz, S., Pastorino, S., 1998. Vegetación del Holoceno en la Cueva Las Buitreras, Santa Cruz, Argentina. Revista Chilena de Historia Natural 71, 277–290.
Reimer, P.J., Brown, T.A., Reimer, R.W., 2004. Discussion: reporting and calibration of post-bomb 14C data. Radiocarbon 46 (3), 1299–1304.
Richter, T.O., van der Gaast, S., Koster, B., Vaars, A., Gieles, R., de Stigter, H.C., de Haas, H., van Weering, T.C.E., 2006. The Avaatech XRF Core Scanner: technical description and applications to NE Atlantic sediments. In: Rothwell, R.G. (Ed.), New Techniques in Sediment Core Analysis. Geological Society Special Publications, London, pp. 39–50.
Round, F.E., Crawford, R.M., Mann, D.G., 1990. The Diatoms. Biology and Morphology of the Genera. Cambridge Univ. Press, Cambridge.
Rumrich, U., Lange-Bertalot, H., Rumrich, M., 2000. Iconographia Diatomologica 9. Diatomeen der Anden (von Venezuela bis Patagonien/Tierra del Fuego). A.R.G. Gantner Verlag, Ruggell.
Sandgren, P., Snowball, I., 2001. Application of mineral magnetic techniques to paleolimnology. In: Last, W.M., Smol, J.P. (Eds.), Tracking Environmental Change Using Lake Sediments. Physical and Geochemical Methods. Tracking Environmental Change Using Lake Sediments, vol. 2. Kluwer Academic Publishers, Dordrecht, pp. 217–237.
Schäbitz, F., Paez, M.M., Mancini, M.V., Quintana, F., Wille, M., Corbella, H., Haberzettl, T., Lücke, A., Prieto, A., Maidana, N., Mayr, C., Ohlendorf, C., Schleser, G.H., Zolitschka, B., 2003. Estudios paleoambientales en lagos volcánicos en la Región Volcánia de Pali Aike, sur de Patagonia (Argentina): palinología. Revista del Museo Argentino de Ciencias Naturales, Nueva Serie 5 (2), 301–316.
Schellmann, G., 1998. Jungkänozoische Landschaftsgeschichte Patagoniens (Argentinien). Essener Geographische Arbeiten, vol. 29. Klartext, Essen. 1–216 pp.
Schneider, C., Glaser, M., Kilian, R., Santana, A., Butorovic, N., Casassa, G., 2003. Weather observations across the southern Andes at 53°S. Physical Geography 24 (2), 97–119.
Simonsen, R., 1987. Atlas and Catalogue of the Diatom Types of Frederich Hustedt. Gebr. Borntraeger, Berlin, Stuttgart.
Stine, S., 1994. Extreme and persistent drought in California and Patagonia during mediaeval time. Nature 369, 546–549.
Stoermer, E.F., 1993. Evaluating diatom succession: some peculiarities of the Great Lakes case. Journal of Paleolimnology 8, 71–83.
Sträßer, M., 1999. Klimadiagramm-Atlas der Erde. Teil 2: Asien, Lateinamerika, Afrika, Australien und Ozeanien. Polarländer, Dortmund.
Stuiver, M., Reimer, P., 1993. Extended 14C database and revised CALIB radiocarbon calibration program. Radiocarbon 35, 215–230.
Stuiver, M., Reimer, P., Reimer, R., 2005. Calib 5.0. [WWW program and documentation].
Tjallingii, R., Röhl, U., Kölling, M., Bickert, T., 2007. Influence of the water content on X-ray fluorescence core-scanning measurements in soft marine sediments. Geochemistry, Geophysics, Geosystems 8 (2), 1–12.
Urrutia, R., Sabbe, K., Cruces, F., Pozo, K., Becerra, J., Araneda, A., Vyverman, W., Parra, O., 2000. Paleolimnological studies of Laguna Chica of San Pedro (VIII Región): diatoms, hydrocarbons and fatty acid records. Revista Chilena de Historia Natural 73 (4), 717–728.
van Dam, H., Mertens, A., Sinkeldam, J., 1994. A coded checklist and ecological indicator values of freshwater diatoms from the Netherlands. Aquatic Ecology 28 (1), 117–133.
Wagner, S., Widmann, M., Jones, J., Haberzettl, T., Lücke, A., Mayr, C., Ohlendorf, C., Schäbitz, F., Zolitschka, B., 2007. Transient simulations, empirical reconstructions and forcing mechanisms for the Mid-Holocene hydrological climate in southern Patagonia. Climate Dynamics 29 (4), 333–355.
Weischet, W., 1996. Regionale Klimatologie. Teil 1: Die Neue Welt: Amerika, Neuseeland, Australien. Teubner Studienbücher der Geographie. Teubner, Stuttgart. 468 pp.
Wenzens, G., 1999. Fluctuations of outlet and valley glaciers in the Southern Andes (Argentina) during the past 13,000 years. Quaternary Research 51, 238–247.
Wenzens, G., 2004. Comment on "modelling the inception of the Patagonian icesheet". Quaternary International 112 (1), 105–109.
Wille, M., Maidana, N.I., Schäbitz, F., Fey, M., Haberzettl, T., Janssen, S., Lücke, A., Mayr, C., Ohlendorf, C., Schleser, G.H., Zolitschka, B., 2007. Vegetation and climate dynamics in southern South America: the microfossil record of Laguna Potrok Aike, Santa Cruz, Argentina. Review of Palaeobotany and Palynology 146, 234–246.
Zolitschka, B., Mingram, J., Van der Gaast, S., Jansen, J.H.F., Naumann, R., 2001. Sediment logging techniques. In: Last, W.M., Smol, J.P. (Eds.), Tracking Environmental Change Using Lake Sediments. Basin Analysis, Coring, and Chronological Techniques, vol. 1. Kluwer Academic Press, Dordrecht, pp. 137–153.
Zolitschka, B., Schäbitz, F., Lücke, A., Corbella, H., Ercolano, B., Fey, M., Haberzettl, T., Janssen, S., Maidana, N., Mayr, C., Ohlen;dorf, C., Oliva, G., Paez, M.M., Schleser, G.H., Soto, J., Tiberi, P., Wille, M., 2006. Crater lakes of the Pali Aike Volcanic Field as key sites for paleoclimatic and paleoecological reconstructions in southern Patagonia, Argentina. Journal of South American Earth Sciences 21 (3), 294–309.